Chemical Science

ROYAL SOCIETY OF CHEMISTRY

EDGE ARTICLE

View Article Online
View Journal | View Issue

Cite this: *Chem. Sci.*, 2021, **12**, 9379

All publication charges for this article have been paid for by the Royal Society of Chemistry

Signature of the neighbor's quantum nuclear dynamics in the electron transfer mediated decay spectra†

Aryya Ghosh,[ab] Lorenz S. Cederbaum *[a] and Kirill Gokhberg[a]

Received 12th March 2021
Accepted 1st June 2021

DOI: 10.1039/d1sc01478a

rsc.li/chemical-science

We computed fully quantum nuclear dynamics, which accompanies electron transfer mediated decay (ETMD) in weakly bound polyatomic clusters. We considered two $HeLi_2$ clusters – with Li_2 being either in the singlet electronic ground state or in the triplet first excited state – in which ETMD takes place after ionization of He. The electron transfer from Li_2 to He^+ leads to the emission of another electron from Li_2 into the continuum. Due to the weak binding of He to Li_2 in the initial states of both clusters, the involved nuclear wavepackets are very extended. This makes both the calculation of their evolution and the interpretation of the results difficult. We showed that despite the highly delocalized nature of the wavepackets the nuclear dynamics in the decaying state is imprinted on the ETMD electron spectra. The analysis of the latter helps understanding the effect which electronic structure and binding strength in the cluster produce on the quantum motion of the nuclei in the decaying state. The results produce a detailed picture of this important charge transfer process in polyatomic systems.

Electron transfer to positive ions in chemical medium can proceed through a variety of processes which involve non-adiabatic effects like the crossing of potential energy surfaces,[1] photon emission,[2–4] or emission of electrons.[5–7] Electron transfer mediated decay or ETMD is a prominent member in the latter group and is most common for singly or multiply charged positive ions, which are produced in clusters or solutions by ionizing radiation.[8–22] It occurs whenever the electron attachment energy of the ion exceeds the threshold for double ionization of the surrounding host matrix. In ETMD, electron transfer from a neighboring atom or molecule to the ion leads to its (partial) neutralization and is accompanied by the emission of another electron from the same (ETMD(2)) or a different (ETMD(3)) neighbor.

To estimate its importance we first notice that from the mechanistic standpoint ETMD is an electronic decay process. Therefore, its lifetimes can be computed using established *ab initio* techniques.[7] They were found to be in the picosecond range for van der Waals clusters,[8,10,13,23] while for hydrated metal cations the lifetime becomes as short as a few tens of femtoseconds.[9,12] As a consequence, if ETMD is energetically allowed, and the ion is in an electronic state for which the other faster electronic decay processes Auger decay or interatomic coulombic decay (ICD) are forbidden, ETMD becomes the leading electron transfer mechanism.[23,24] To date it has been experimentally observed in clusters or solutions, where the ion was prepared in the ground or a low-lying electronic state.[15–22]

ETMD can be seen as incorporating two familiar processes – charge transfer and ionization. Therefore, it is a pathway to either partial neutralization of a cation or double ionization of atoms or molecules in its vicinity. As we demonstrate in our article, by doubly ionizing a molecular neighbor, ETMD can lead to the breaking of covalent bonds. Thus, in aqueous solutions ETMD was shown to efficiently produce radical species by ionizing water molecules,[9,12,20] which dissociate as the result. The produced radicals undergo reactions with other molecules present in the vicinity. Radiative damage to DNA is caused by slow electrons and radical species formed in its vicinity.[25] ETMD is an efficient process producing such electrons and radicals.

ETMD has been also utilized to produce and study the properties of dications embedded in He nanodroplets. Such droplets are known to serve as 'refrigerators' for the immersed dopants.[26] Following ionization of He, ETMD takes place with the resulting He^+ producing a dication of the dopant which is efficiently cooled and stabilized by the He-matrix. The technique was used to study stability of small doubly charged Mg clusters.[17] The formation of dications and the investigation of their stability have been reported in experiments on alkali[27] and coronene clusters[28] in He_n. Reactions involving molecular dications are of general interest. They occur even under the extreme conditions of the interstellar medium and are

[a]*Theoretische Chemie, Physikalisch-Chemisches Institut, Universität Heidelberg, Im Neuenheimer Feld 229, D-69120 Heidelberg, Germany. E-mail: lorenz.cederbaum@pci.uni-heidelberg.de*

[b]*Department of Chemistry, Ashoka University, Sonipat, India*

† Electronic supplementary information (ESI) available. See DOI: 10.1039/d1sc01478a

responsible for the appearance of polyatomic molecules in the space.[29] They can be modeled in doped He nanodroplets, as was demonstrated in the case of the C_{60}–H_2O cluster.[30]

Generation of positive ions in van der Waals clusters or in solutions *via* photon absorption or charged particle impact is nearly sudden, and leads to highly non-equilibrium nuclear configurations. Since the ETMD lifetimes at these geometries are usually comparable or longer than the characteristic vibrational periods in the ion-neighbor modes, it is usually accompanied by vibrational motion. Computations in atomic van der Waals clusters show[10,13] that vibrational motion, which follows ionization of some atom, tends on average to decrease the distance between the resulting ion and its neighbors and leads to the shortening of the effective ETMD lifetimes by as much as an order of magnitude. As a consequence, the spectra of ETMD electrons differ from the spectra which would be obtained at fixed nuclei.[13] Importantly, in dimers the vibrational wavepacket is imprinted onto the electron or kinetic energy release of the nuclei (KER) spectra, if the potential energy curve of the final state is repulsive, and the dimer disintegrates at the end of the process.[13] This is a common feature in interatomic electronic decay of diatomic clusters.[31] It was used to predict and observe the vibrational wave functions in highly excited He_2^+ which underwent ICD.[32] Coupled with ingenious timing techniques such as post collision interaction (PCI) clock,[33] this feature was used to experimentally reconstruct the wave packet evolution during ICD in rare gas dimers.[34]

In ETMD in atomic van der Waals dimers the wave packet evolves over the entire potential energy curve. Since the decay width decreases exponentially with the interatomic distance,[8,13,23] ETMD occurs predominantly at the inner repulsive wall.[13] This picture simplifies the qualitative analysis of ETMD spectra in dimers. However, no numerical results and no similar picture exist for ETMD in clusters of more than two atoms, due to the complexity of the necessary computations. It becomes more difficult to obtain highly energetic potential energy surfaces (PES) of the decaying electronic states in more than one dimension and calculate the respective position dependent decay widths. Moreover, already for a triatomic system one needs to consider the dynamics of three coupled vibrational modes in the decaying and final states over an extended spatial range. This situation in theory is mirrored by the one in experiment, where ETMD was observed either in dimers or in large clusters but not in trimers.

In this letter we present for the first time the computational results of the full quantum dynamics during ETMD in a triatomic system. Here we choose the $HeLi_2$ cluster which is a basic unit suggested by the experiments on ionization of helium droplets doped with alkali dimers.[22] A particular property of these systems is that the alkali dimers can be produced on the surface of a droplet in two different electronic states – the singlet ground state $^1\Sigma_g^+$ or the triplet first excited state $^3\Sigma_u^+$ – which have widely different binding properties. Thus, $Li_2(^1\Sigma_g^+)$ is a molecule with binding energy of 1 eV, while $Li_2(^3\Sigma_u^+)$ is itself a weakly bound (41 meV) dimer held together by a van der Waals force.[35] Correspondingly, following the ionization of He, the $HeLi_2(^1\Sigma_g^+)$ and $HeLi_2(^3\Sigma_u^+)$ clusters are expected to undergo ETMD(2) and ETMD(3) respectively. It is the goal of this investigation to uncover the differences in the quantum nuclear dynamics which accompanies these processes and to relate them to the differences in the observable spectra.

The following equation summarizes the decay process

$$He^+Li_2 \rightarrow HeLi^+Li^+ + e_{ETMD}, \quad (1)$$

after which the cluster disintegrates either completely, forming He and two Li^+ ions, or into the $HeLi^+$ and Li^+ fragments. We computed and discussed the *ab initio* potential energy surfaces and decay widths in ref. 36, where all structural and energetics data can be found. Here we would only like to make a few remarks important for the following discussion. First, the binding of He to Li_2 in the initial state is extremely weak. The distance between He and the center of mass of Li_2 is 6.9 Å and 5.4 Å for the singlet and triplet states, respectively, and the respective He–Li_2 binding energies are less than 1 meV. As the result, the nuclear wavefunction Ψ_i of the initial electronic state is strongly delocalized along the He–Li_2 coordinate. This complicates the calculations, since very large grids, which extend up to 50 Å, are needed in the respective coordinate for propagating the wavepacket. Second, the equilibrium geometry in the decaying He^+Li_2 state is very different from the one in the respective initial state. Therefore, sudden ionization of the cluster populates a band of highly excited vibrational states on the decaying PES. Third, the ETMD lifetimes at the equilibrium geometries of the initial states are very long (130 ps and 220 ps for the singlet and triplet states, respectively). This, together with the point two above, explains why extensive nuclear motion occurs during the decay.

To analyse the nuclear dynamics and to compute the energies of ETMD electrons we numerically solved the following system of equations for the vibrational wavepackets $|\Psi_d(t)\rangle$ and $|\Psi_f(E,t)\rangle$ in the decaying and final states[37,38]

$$i\left|\dot{\Psi}_d(t)\right\rangle = \left(\hat{T}_N + \hat{V}_d - \frac{i}{2}\hat{\Gamma}\right)|\Psi_d(t)\rangle$$
$$i\left|\dot{\Psi}_f(t)\right\rangle = \left(\hat{T}_N + \hat{V}_f + E\right)|\Psi_f(E,t)\rangle + \hat{W}_f|\Psi_d(t)\rangle \quad (2)$$

by using the multiconfiguration time-dependent Hartree (MCTDH) method.[39,40] The $\hat{T}_N$ operator is the operator of the kinetic energy of the nuclei, while $\hat{V}_d$ and $\hat{V}_f$ operators are respectively the PES of the decaying and the final state f, and E is the energy of the emitted ETMD electron. The quantities $\hat{W}_f$ and $\hat{\Gamma}$ are the ETMD amplitude for the transition to the final state f and the total decay width, which is obtained by summing over all final states accessible from the decaying state. In our case ETMD and radiative charge transfer or RCT[3,4] are the only possible decay processes, and RCT is several orders of magnitude slower than ETMD.[4,23] Neglecting its contribution to the total width and taking into account that for the cluster in question there is a single ETMD final state we find $\Gamma = 2\pi|\hat{W}_f|^2$.

The PES, decay amplitude and width are functions of nuclear coordinates **Q**. For the system in question we used the Jacobi coordinates R, r, and θ, which stand respectively for the distance

from He to the Li_2 center of mass, Li–Li distance, and the angle between the Li_2 molecular axis and the line connecting He with the center of mass of Li_2 (see Fig. 1 in the ESI†). Assuming instantaneous ionization of the cluster we set $|\Psi_d(t=0)\rangle = |\Psi_i\rangle$ and $|\Psi_f(E,t=0)\rangle = 0$, where $|\Psi_i\rangle$ is the vibrational ground state in the initial electronic state of the respective cluster. To avoid wavepacket reflection from the end of the grid we employed cubic complex absorbing potential (CAP). We used the wavepacket $|\Psi_d(t)\rangle$ to analyse the nuclear motion in the decaying state and to estimate the ETMD lifetime from the respective survival probability. The wavepacket $|\Psi_f\rangle(E,t)$ is used for computing the electron spectrum as observed either at some time instant t or at some very long time when the decay is essentially over

$$\sigma(E,t) = \langle \Psi_f(E,t) | \Psi_f(E,t) \rangle$$
$$\sigma(E) = \lim_{t\to\infty} \sigma(E,t) \quad (3)$$

We solved the equations and computed the spectra both on the full three-dimensional and reduced two-dimensional PES of $HeLi_2$. The complete list of technical details of the MCTDH calculations is given in the ESI.†

Strong delocalization of the initial wavefunction precludes the analysis of the dynamics in the decaying state in terms of moving wavepackets. However, information about the evolution of the vibrational state can be obtained from the behavior of the survival probability $\langle \Psi_d(t) | \Psi_d(t) \rangle$ with time. We found that in the $HeLi_2(^1\Sigma_g^+)$ cluster up to $t = 15$ ps it decays nearly exponentially with the lifetime $\tau = 12$ ps.[41] Beyond that time while the decay remains nearly exponential the lifetime τ increases to 17 ps. Additional analysis of the survival probability with Γ set to zero in eqn (2) led to the following picture of the events. In the ionization event the vertical transition of the delocalized initial wavefunction $\Psi_i(\mathbf{Q})$ to the PES of the decaying state populates vibrational states which lie both below and above the He^+/Li_2 dissociation threshold. In the nuclear dynamics which follows, He^+ is first pulled towards and collides with Li_2. Whereupon the continuum part of the wavepacket propagates outwards along the coordinate R until it reaches the CAP and is absorbed by it, while the bound part remains trapped in the potential and decays by ETMD.

The shorter lifetime of $|\Psi_d(t)\rangle$ at the times below 15 ps reflects both the electronic decay *via* ETMD, and the dissociation of a part of He^+Li_2 clusters into the He^+/Li_2 channel. The longer decay lifetime beyond 15 ps reflects only the ETMD of the remaining bound $He^+Li_2(^1\Sigma_g^+)$ clusters. While it is difficult to compute the accurate ETMD-to-dissociation branching ratio, our calculations show that up to 30% of $HeLi_2(^1\Sigma_g^+)$ clusters would dissociate following the ionization of He in the absence of ETMD. Similar picture holds for the $HeLi_2(^3\Sigma_u^+)$ clusters, although a larger proportion (57% in the absence of ETMD) of them dissociates after sudden ionization of He due to the breaking of the much weaker Li–Li bond. We also estimated the effective lifetime of $He^+Li_2(^1\Sigma_g^+)$ clusters due to ETMD alone as 19.8 ps, while for the $He^+Li_2(^3\Sigma_u^+)$ clusters it is 21.5 ps. The difference between them is insignificant, so that the electronic structure of the cluster has little effect on the overall decay rate. However, nuclear dynamics leads to effective ETMD lifetimes which are almost an order of magnitude shorter than the purely electronic lifetimes corresponding to the equilibrium geometries in the initial state.

More information about the dynamics can be derived from the ETMD electron spectra of the respective singlet and triplet $HeLi_2$ clusters. The emitted electron spectrum which results from the decay of the $He^+Li_2(^1\Sigma_g^+)$ state is shown in Fig. 1. The ETMD peak is located between 7 eV and 8 eV. Its position coincides with the interval (6.8 eV to 7.8 eV) of expected ETMD electron energies, which we estimated from purely electronic considerations in the previous publication.[36] There we assumed that the decay predominantly occurs at the configurations of the nuclei where two conditions are fulfilled: the relative velocities of the nuclei are small and the ETMD rate is large. We also kept the Li–Li distance r constant, under assumption that it would not change much in the strongly bound $Li_2(^1\Sigma_g^+)$ state. While this simple model works surprisingly well in estimating the position and width of the ETMD peak, it fails to reproduce the

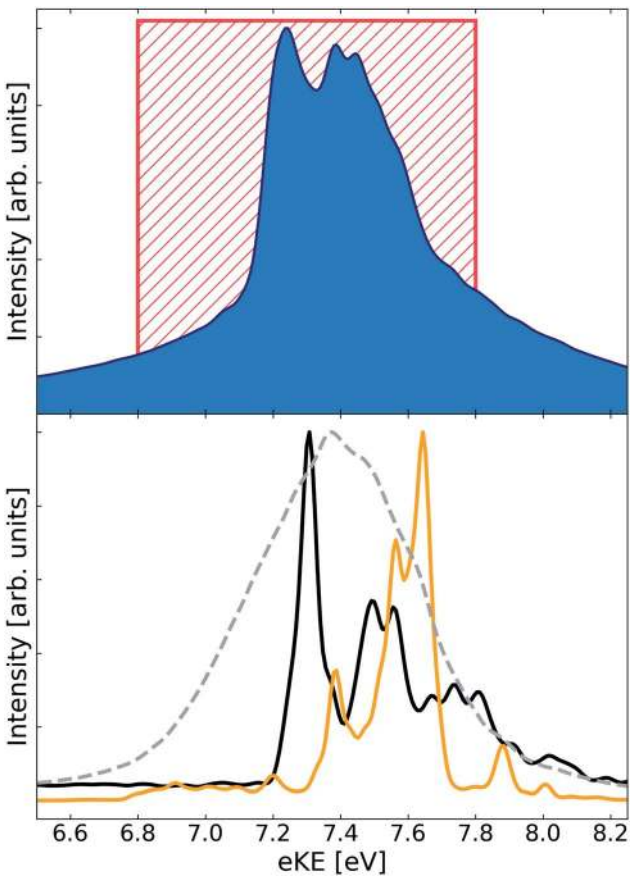

Fig. 1 ETMD electron spectra obtained following the ionization of He in the $He–Li_2(^1\Sigma_g^+)$ cluster. (upper panel) Electron spectrum obtained following wavepacket propagation on the full three-dimensional surface of the decaying state. Red rectangle shows the position of the peak as estimated from electronic properties in ref. 36. (lower panel) Electronic spectra obtained following wavepacket propagation on reduced two-dimensional surfaces of the decaying state. Green line – propagation on the 2D-cut (R, r, $\theta = 0$); red line – propagation on the 2D-cut (R, r, $\theta = \pi/2$); broken gray line – propagation on the 2D-cut (R, θ, $r = r_{eq}$). All spectra are scaled to have the same absolute maximum.

main finding of the full dynamics, namely, that the spectrum exhibits structure despite the strongly delocalized nuclear wavepacket involved. We observe peaks at 7.24 eV, 7.39 eV, 7.44 eV and a shoulder at 7.58 eV. The distances between the nearest peaks vary between 50 meV and 150 meV. To trace their origin we can compare these numbers with some characteristic frequencies in our system. The fundamental frequencies of $Li_2(^1\Sigma_g^+)$ and in the electronic ground state of He^+Li (a possible product) are 42 meV (10.2 THz) and 30 meV (7.3 THz), while the fundamental frequency in the R-mode in He^+–Li_2 is 32 meV (7.7 THz). None of these numbers can adequately explain the progression observed in the spectrum.

To clarify how the vibrational structure comes about we computed ETMD spectra by running nuclear dynamics on three reduced two-dimensional surfaces of the decaying state. First, we kept the Li–Li distance r fixed at the equilibrium distance r_{eq} = 2.69 Å of the $Li_2(^1\Sigma_g^+)$ so that He^+ moves around and collides with rigid Li_2. The resulting spectrum is shown as the broken line in Fig. 1. It appears as a single peak whose position and width coincide with those of the peak in the full three-dimensional spectrum. However, it lacks any vibrational structure observed in the latter. Keeping θ fixed but allowing vibrational motion along the Li–Li coordinate r leads to a dramatic change in the spectral shape. The spectra computed at $\theta = 0$ and $\theta = \pi/2$ lie both in the same energy window as the spectrum obtained at constant r. However, while the former is a broad featureless peak, the latter two appear as vibrational progressions. The spectrum at $\theta = \pi/2$ shows peaks with spacings between them being between 80 meV to 180 meV. The spectrum at $\theta = 0$ appears mostly as three peaks spaced by about 200 meV; two of these peaks are in turn split into peaks separated by about 50 meV. Importantly, one can see the correspondence between the peaks in the full spectrum and the structure in the spectra obtained on these reduced 2D surfaces. For example, the leftmost peak at 7.24 eV originates from the leftmost peak (7.31 eV) of the $\theta = 0$ spectrum; likewise, the shoulder at 7.58 eV corresponds to the pronounced peak at 7.64 eV in the $\theta = \pi/2$ spectrum. The peaks between these two extremes can be also recognized in the two-dimensional spectra.

Consequently, the vibrational structure in the ETMD electron spectra of the $He^+Li_2(^1\Sigma_g^+)$ state can be traced to the vibration of the Li_2 molecule. The remaining question is why the spacing between the peaks both in the full and reduced two-dimensional spectra at fixed θ is larger than characteristic vibrational frequencies in the decaying or the final states. One arrives at a plausible answer if one follows the chain of processes set off by sudden ionization of He. The appearance of the positive charge on He leads to the change in the Li–Li interaction potential. This change becomes more pronounced as the He–Li_2 distance R decreases.[36] The sudden perturbation of Li_2 due to ionization of He, and the transfer of vibrational energy from the He–Li_2 mode during the dynamics that follows lead to the population of excited states in the Li–Li mode. The final state PES, V_f, is repulsive along the coordinate r and behaves nearly as $1/r$. Therefore, changing r at which the decay occurs by 0.1 Å about r_{eq} = 2.69 Å shifts the energy of emitted electrons by 200 meV. On the contrary, the energy of the emitted electrons is less sensitive to changes in the coordinates R and θ. Thus, the vibrational progression in the ETMD electron spectra in Fig. 1 is the imprint of the vibrational wavepacket in the Li–Li mode. This conclusion is supported by the analysis of the vibrational eigenfunctions, $\phi_n(r)$, of the $Li_2(^1\Sigma_g^+)$ molecule. Indeed, the distance between the nearest maxima of the $|\phi_n(r)|^2$ varies between 0.23 Å for $n = 3$ to 0.15 Å for $n = 10$; the projection of these states onto the repulsive Li^+–Li^+ potential curve would result in the peaks in electron spectra separated by a few hundred meV. This picture of a triatomic cluster is the generalization of observations made in the previous *ab initio* computations and experiments in diatomic clusters, which demonstrated that electronic decay onto repulsive potential energy curve imprinted the vibrational structure of the decaying state onto the spectra of emitted electrons or kinetic energy release of the nuclei.[31,32,34,42]

The electron spectra arising from the decay of $He^+Li_2(^3\Sigma_u^+)$ are shown in Fig. 2. The ETMD peak is located between 7.75 eV and

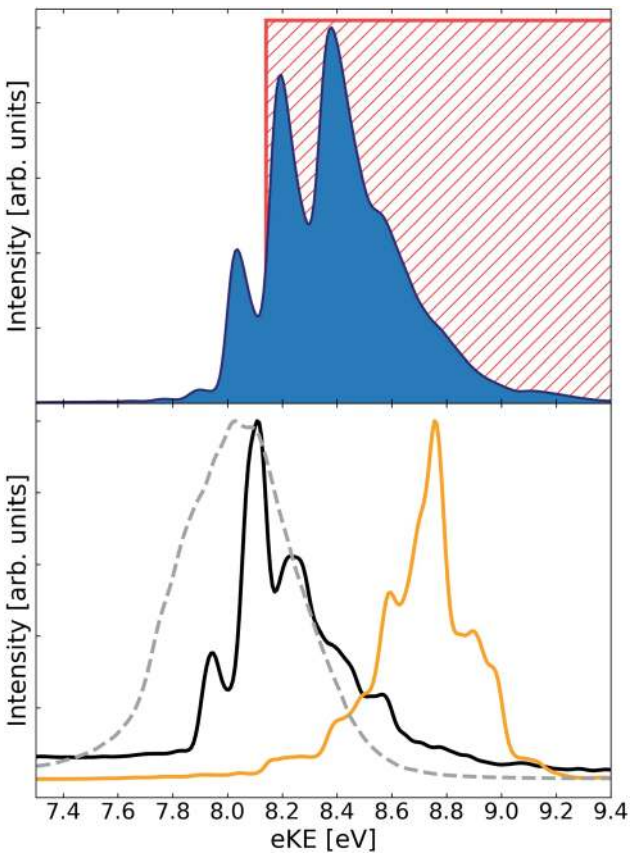

Fig. 2 ETMD electron spectra obtained following the ionization of He in the He–$Li_2(^3\Sigma_u^+)$ cluster. (upper panel) Electronic spectrum obtained following wavepacket propagation on the full three-dimensional surface of the decaying state. Red rectangle shows the position of the peak as estimated from the potential energy surfaces at the T-shaped geometry of the cluster (see ref. 36). (lower panel) Electronic spectra obtained following wavepacket propagation on reduced two-dimensional surfaces of the decaying state. Green line – propagation on the 2D-cut (R, r, $\theta = 0$); red line – propagation on the 2D-cut (R, r, $\theta = \pi/2$); broken gray line – propagation on the 2D-cut (R, θ, $r = r_{eq}$). All spectra are scaled to have the same absolute maximum.

9.25 eV. The full spectrum fits less well to the range of electron energies (8.1 eV to 10.2 eV) we determined previously using a simple model similar to the one explained above for the singlet cluster. The only difference between the models was that in the case of the triplet cluster we kept the angle $\theta = \pi/2$ constant and not the Li–Li distance r. Although unexpected, due to the weak Li–Li bond, the spectrum again shows a pronounced structure with peaks at 8.04 eV, 8.20 eV, 8.38 eV and a shoulder at 8.56 eV. As in the case of the $He^+Li_2(^1\Sigma_g^+)$ cluster the spectrum obtained when keeping the Li–Li distance, r, fixed at the respective equilibrium distance appears as a featureless peak. It is relaxing r that leads to the structure appearing in the electron spectrum.

It is interesting to compare the spectra of the two systems, which represent two classes of clusters: a molecule–atom cluster ($HeLi_2(^1\Sigma_g^+)$), and a triatomic van der Waals cluster ($HeLi_2(^3\Sigma_u^+)$). The first obvious difference is how well the electron spectra obtained for the reduced two-dimensional PES match the respective full spectra. In the case of the $HeLi_2(^1\Sigma_g^+)$ cluster the three spectra on different reduced surfaces lie within the envelope of the full spectrum. Moreover, there is strong overlap between the full spectrum and the spectra when θ is held constant at 0 and $\pi/2$. This indicates that He^+ moves around Li_2 unhindered and explores the regions characterized by different values of θ with comparable probabilities. In addition, the peaks in the full spectrum correspond to the peaks in spectra obtained at constant θ, and can be related to the vibrational excitations in the Li–Li mode. These results confirm our assumption of an ETMD(2) process between He^+ and Li_2 in the $HeLi_2(^1\Sigma_g^+)$ cluster. They also explain the excellent correspondence between the computed spectrum and the range of energies of the emitted electrons found assuming rigid Li_2 (see Fig. 1).

In the case of the $HeLi_2(^3\Sigma_u^+)$ cluster only one of the spectra obtained on the reduced surfaces ($\theta = 0$) overlaps strongly with the full spectrum. In addition, it becomes more difficult to relate the latter's structure to the peaks in spectra obtained at $\theta = 0$ and $\theta = \pi/2$. This indicates a breakdown of the atom–molecule model, which worked well in the previous case. Indeed, one would expect the effect of the ionization of He and the subsequent dynamics to be sufficient for breaking the weak Li–Li bond. Thus, the structure in the electron spectra, while carrying the image of the vibrational wavepacket reflected in the dissociative final state PES, cannot be interpreted as arising through the vibrationally excited Li_2 molecule. It seems, that in the weakly bound triatomic $HeLi_2(^3\Sigma_u^+)$ cluster all degrees of freedom are equally important in shaping the ETMD electron spectrum, as one would expect for an ETMD(3) process. The structure seen in the spectrum is most probably due to interference effects in the dynamics of an enormously extended wavepacket.

In conclusion, we computed nuclear dynamics which accompanies electronic transfer mediated decay (ETMD) in different metastable electronic states of the weakly bound triatomic $HeLi_2$ cluster. The computations were made particularly challenging by the necessity to compute quantum dynamics on three-dimensional complex surfaces of the decaying states, and by the enormous extent of the wavepackets due to the extremely weak binding of Li_2 to He in the initial states. We showed that the nuclear wavepacket which evolves on the PES of the ETMD state following the ionization of He is imprinted on the ETMD electron spectra. This becomes possible since the potential energy surface of the final state is repulsive along the Li–Li coordinate. Due to the extremely weak binding of He to Li_2 and strong delocalization of the wavepackets, no semiclassical description of the dynamics is possible. However, the analysis of the spectra helps understanding how the nuclear motion in the decaying state depends on the electronic structure and binding in the cluster. In $HeLi_2(^1\Sigma_g^+)$, where Li–Li bond is strong, the dynamics is dominated by the motion of He^+ around the Li_2 molecule. The vibrational excitation of Li_2 – which occurs both in the sudden ionization of He and through the energy transfer from other modes during the dynamics – appears as a characteristic structure in the electronic peak. In the $HeLi_2(^3\Sigma_u^+)$ cluster the weak Li–Li bond is quickly broken and contributions of dynamics in different modes to the electron spectrum cannot be disentangled. Surprisingly, the spectrum still carries the imprint of the vibrational motion, which disappears if we freeze the dynamics along the Li–Li coordinate.

The effects described in this work can be observed in other experimentally realizable systems. Suitable candidates are the rare-gas trimers $NeXe_2$ and $NeKr_2$. After core ionization of Ne, a fast Auger decay takes place producing of $Ne^{2+}(2p^{-2})$ cations. The ETMD(3) channel is open in these rare-gas trimers as has been shown before.[10,13] Another system of potential interest to experimentalists is Ne–H_2O. Despite the high double ionization potential of water ($\approx$39 eV (ref. 43)), the ETMD channel is open in the Franck–Condon region for the $Ne^{2+}(2p^{-2}\ ^1S)$ state. Following ETMD, the doubly ionized H_2O would dissociate in a number of channels like OH^+/H^+ or $2H^+/O$ along strongly repulsive potential surfaces[44] such that the signature of the vibrational motion of water can be observed in the ETMD spectra. Importantly, water fragmentation and KER of ions in different dissociation channels were investigated experimentally for the one-photon double ionization of water monomer.[45] This also offers an opportunity to compare the KER in the same dicationic states of water produced *via* different double ionization mechanisms. The simpler systems studied in this letter can thus serve as a model for the ETMD(2) and ETMD(3) processes in such ion–molecule or weakly bound atomic clusters.

Data availability

Additional data are available on request.

Author contributions

AG and KG carried out the calculations. All authors equally contributed to writing the article.

Conflicts of interest

There are no conflicts to declare.

Acknowledgements

The authors would like to thank Dieter Meyer and Markus Schröder for their help with the Heidelberg MCTDH package. Financial support by the European Research Council (ERC) (Advanced Investigator Grant No. 692657) is gratefully acknowledged.

References

1 H. Nakamura, Semiclassical approach to charge-transfer processes in ion-molecule collisions, in *Advances in Chemical Physics*, John Wiley & Sons, Ltd, 1992, pp. 243–319.
2 R. Johnsen and M. A. Biondi, Measurements of radiative charge-transfer reactions of doubly and singly charged rare-gas ions with rare-gas atoms at thermal energies, *Phys. Rev. A: At., Mol., Opt. Phys.*, 1978, **18**, 996–1003.
3 N. Saito, Y. Morishita, I. Suzuki, S. Stoychev, A. Kuleff, L. Cederbaum, X.-J. Liu, H. Fukuzawa, G. Prümper and K. Ueda, Evidence of radiative charge transfer in argon dimers, *Chem. Phys. Lett.*, 2007, **441**, 16–19.
4 A. Hans, V. Stumpf, X. Holzapfel, F. Wiegandt, P. Schmidt, C. Ozga, P. Reiß, L. B. Ltaief, C. Küstner-Wetekam, T. Jahnke, A. Ehresmann, P. V. Demekhin, K. Gokhberg and A. Knie, Direct evidence for radiative charge transfer after inner-shell excitation and ionization of large clusters, *New J. Phys.*, 2018, **20**, 012001.
5 R. Carmina Monreal, Auger neutralization and ionization processes for charge exchange between slow noble gas atoms and solid surfaces, *Prog. Surf. Sci.*, 2014, **89**, 80–125.
6 A. B. Voitkiv, Transfer ionization in collisions with a fast highly charged ion, *Phys. Rev. Lett.*, 2013, **111**, 043201.
7 T. Jahnke, U. Hergenhahn, B. Winter, R. Dörner, U. Frühling, P. V. Demekhin, K. Gokhberg, L. S. Cederbaum, A. Ehresmann, A. Knie and A. Dreuw, Interatomic and Intermolecular Coulombic Decay, *Chem. Rev.*, 2020, **120**, 11295.
8 J. Zobeley, R. Santra and L. S. Cederbaum, Electronic decay in weakly bound heteroclusters: energy transfer versus electron transfer, *J. Chem. Phys.*, 2001, **115**, 5076.
9 I. B. Müller and L. S. Cederbaum, Electronic decay following ionization of aqueous Li+ microsolvation clusters, *J. Chem. Phys.*, 2005, **122**, 094305.
10 V. Stumpf, P. Kolorenč, K. Gokhberg and L. S. Cederbaum, Efficient pathway to neutralization of multiply charged ions produced in Auger processes, *Phys. Rev. Lett.*, 2013, **110**, 258302.
11 J. P. Zobel, N. V. Kryzhevoi and M. Pernpointner, Communication: electron transfer mediated decay enabled by spin-orbit interaction in small krypton/xenon clusters, *J. Chem. Phys.*, 2014, **140**, 161103.
12 V. Stumpf, K. Gokhberg and L. S. Cederbaum, The role of metal ions in X-ray-induced photochemistry, *Nat. Chem.*, 2016, **8**, 237.
13 V. Stumpf, S. Scheit, P. Kolorenč and K. Gokhberg, Electron transfer mediated decay in NeXe triggered by K-LL Auger decay of Ne, *Chem. Phys.*, 2017, **482**, 192.
14 E. Fasshauer, M. Förstel, M. Mucke, T. Arion and U. Hergenhahn, Theoretical and experimental investigation of Electron Transfer Mediated Decay in ArKr clusters, *Chem. Phys.*, 2017, **482**, 226.
15 M. Förstel, M. Mucke, T. Arion, A. M. Bradshaw and U. Hergenhahn, Autoionization mediated by electron transfer, *Phys. Rev. Lett.*, 2011, **106**, 033402.
16 K. Sakai, S. Stoychev, T. Ouchi, I. Higuchi, M. Schöffler, T. Mazza, H. Fukuzawa, K. Nagaya, M. Yao, Y. Tamenori, A. I. Kuleff, N. Saito and K. Ueda, Electron-transfer-mediated decay and interatomic coulombic decay from the triply ionized states in argon dimers, *Phys. Rev. Lett.*, 2011, **106**, 033401.
17 A. C. LaForge, V. Stumpf, K. Gokhberg, J. von Vangerow, F. Stienkemeier, N. V. Kryzhevoi, P. O'Keeffe, A. Ciavardini, S. R. Krishnan, M. Coreno, K. C. Prince, R. Richter, R. Moshammer, T. Pfeifer, L. S. Cederbaum and M. Mudrich, Enhanced Ionization of Embedded Clusters by Electron-Transfer-Mediated Decay in Helium Nanodroplets, *Phys. Rev. Lett.*, 2016, **116**, 203001.
18 T. Ouchi, H. Fukuzawa, K. Sakai, T. Mazza, M. Schöffler, K. Nagaya, Y. Tamenori, N. Saito and K. Ueda, Interatomic coulombic decay and electron-transfer-mediated decay following triple ionization of Ne2 and NeAr, *Chem. Phys.*, 2017, **482**, 244.
19 D. You, H. Fukuzawa, Y. Sakakibara, T. Takanashi, Y. Ito, G. G. Maliyar, K. Motomura, K. Nagaya, T. Nishiyama, K. Asa, Y. Sato, N. Saito, M. Oura, M. Schöffler, G. Kastirke, U. Hergenhahn, V. Stumpf, K. Gokhberg, A. I. Kuleff, L. S. Cederbaum and K. Ueda, Charge transfer to ground-state ions produces free electrons, *Nat. Commun.*, 2017, **8**, 14277.
20 I. Unger, R. Seidel, S. Thürmer, M. N. Pohl, E. F. Aziz, L. S. Cederbaum, E. Muchová, P. Slavíček, B. Winter and N. V. Kryzhevoi, Observation of electron-transfer-mediated decay in aqueous solution, *Nat. Chem.*, 2017, **9**, 708.
21 M. N. Pohl, C. Richter, E. Lugovoy, R. Seidel, P. Slavíček, E. F. Aziz, B. Abel, B. Winter and U. Hergenhahn, Sensitivity of Electron Transfer Mediated Decay to Ion Pairing, *J. Phys. Chem. B*, 2017, **121**, 7709.
22 L. B. Ltaief, M. Shcherbinin, S. Mandal, S. R. Krishnan, R. Richter, T. Pfeifer, M. Bauer, A. Ghosh, M. Mudrich, K. Gokhberg and A. LaForge, Electron transfer mediated decay of alkali dimers attached to He nanodroplets, *Phys. Chem. Chem. Phys.*, 2020, **22**, 8557.
23 V. Stumpf, N. V. Kryzhevoi, K. Gokhberg and L. S. Cederbaum, Enhanced one-photon double ionization of atoms and molecules in an environment of different species, *Phys. Rev. Lett.*, 2014, **112**, 193001.
24 V. Averbukh and L. S. Cederbaum, "Ab initio calculation of interatomic decay rates by a combination of the Fano ansatz, Green's-function methods, and the Stieltjes imaging technique, *J. Chem. Phys.*, 2005, **123**, 204107.
25 E. Alizadeh, T. M. Orlando and L. Sanche, Biomolecular Damage Induced by Ionizing Radiation: The Direct and Indirect Effects of Low-Energy Electrons on DNA, *Annu. Rev. Phys. Chem.*, 2015, **66**, 379.

26 S. Yang and A. M. Ellis, Helium droplets: a chemistry perspective, *Chem. Soc. Rev.*, 2013, **42**, 472–484.
27 M. Mahmoodi-Darian, S. Raggl, M. Renzler, M. Goulart, S. E. Huber, A. Mauracher, P. Scheier and O. Echt, Doubly charged coronene clusters—much smaller than previously observed, *J. Chem. Phys.*, 2018, **148**, 174303.
28 M. Renzler, M. Harnisch, M. Daxner, L. Kranabetter, M. Kuhn, P. Scheier and O. Echt, Fission of multiply charged alkali clusters in helium droplets – approaching the Rayleigh limit, *Phys. Chem. Chem. Phys.*, 2016, **18**, 10623–10629.
29 D. K. Böhme, Multiply-charged ions and interstellar chemistry, *Phys. Chem. Chem. Phys.*, 2011, **13**, 18253–18263.
30 S. Denifl, F. Zappa, I. Mähr, F. Ferreira da Silva, A. Aleem, A. Mauracher, M. Probst, J. Urban, P. Mach, A. Bacher, O. Echt, T. Märk and P. Scheier, Ion–molecule reactions in helium nanodroplets doped with c60 and water clusters, *Angew. Chem.*, 2009, **48**, 8940–8943.
31 N. Moiseyev, R. Santra, J. Zobeley and L. S. Cederbaum, Fingerprints of the nodal structure of autoionizing vibrational wave functions in clusters: interatomic coulombic decay in Ne dimer, *J. Chem. Phys.*, 2001, **114**, 7351.
32 N. Sisourat, N. V. Kryzhevoi, P. Kolorenč, S. Scheit, T. Jahnke and L. S. Cederbaum, Ultralong-range energy transfer by interatomic coulombic decay in an extreme quantum system, *Nat. Phys.*, 2010, **6**, 508.
33 U. Frühling, F. Trinter, F. Karimi, J. B. Williams and T. Jahnke, Time-resolved studies of interatomic coulombic decay, *J. Electron Spectrosc. Relat. Phenom.*, 2015, **204**, 237–244.
34 F. Trinter, J. B. Williams, M. Weller, M. Waitz, M. Pitzer, J. Voigtsberger, C. Schober, G. Kastirke, C. Müller, C. Goihl, P. Burzynski, F. Wiegandt, T. Bauer, R. Wallauer, H. Sann, A. Kalinin, L. Schmidt, M. Schöffler, N. Sisourat and T. Jahnke, Evolution of Interatomic Coulombic Decay in the Time Domain, *Phys. Rev. Lett.*, 2013, **111**, 093401.
35 M. Musiał and S. A. Kucharski, First principle calculations of the potential energy curves for electronic states of the lithium dimer, *J. Chem. Theory Comput.*, 2014, **10**, 1200–1211.
36 A. Ghosh, L. S. Cederbaum and K. Gokhberg, Electron transfer mediated decay in $HeLi_2$ cluster: potential energy surfaces and decay widths, *J. Chem. Phys.*, 2019, **150**, 164309.
37 L. S. Cederbaum and F. Tarantelli, Nuclear dynamics of decaying states: a time-dependent formulation, *J. Chem. Phys.*, 1993, **98**, 9691–9706.
38 E. Pahl, H.-D. Meyer and L. Cederbaum, Competition between excitation and electronic decay of short-lived molecular states, *Z. Phys. D: At., Mol. Clusters*, 1996, **38**, 215–232.
39 H.-D. Meyer, U. Manthe and L. Cederbaum, The multi-configurational time-dependent Hartree approach, *Chem. Phys. Lett.*, 1990, **165**, 73–78.
40 M. Beck, A. Jäckle, G. Worth and H.-D. Meyer, The multiconfiguration time-dependent Hartree (MCTDH) method: a highly efficient algorithm for propagating wavepackets, *Phys. Rep.*, 2000, **324**, 1–105.
41 Electronic decay of an isolated resonance will proceed exponentially in time apart from very short or very long times, in our case, a band of vibronic states with close but different widths decay simultaneuosly. Still, the log–linear plot of the survival probability appears very much like a straight line.
42 T. Miteva, Y.-C. Chiang, P. Kolorenč, A. I. Kuleff, K. Gokhberg and L. S. Cederbaum, Interatomic coulombic decay following resonant core excitation of Ar in argon dimer, *J. Chem. Phys.*, 2014, **141**, 064307.
43 I. B. Müller and L. S. Cederbaum, Ionization and double ionization of small water clusters, *J. Chem. Phys.*, 2006, **125**, 204305.
44 Z. L. Streeter, F. L. Yip, R. R. Lucchese, B. Gervais, T. N. Rescigno and C. W. McCurdy, Dissociation dynamics of the water dication following one-photon double ionization. i. Theory, *Phys. Rev. A*, 2018, **98**, 053429.
45 D. Reedy, J. B. Williams, B. Gaire, A. Gatton, M. Weller, A. Menssen, T. Bauer, K. Henrichs, P. Burzynski, B. Berry, Z. L. Streeter, J. Sartor, I. Ben-Itzhak, T. Jahnke, R. Dörner, T. Weber and A. L. Landers, Dissociation dynamics of the water dication following one-photon double ionization. ii. Experiment, *Phys. Rev. A*, 2018, **98**, 053430.